Please cite the Published Version

Data Access Statement: Data will be made available on request.

1 **TITLE:**

2 Practical Limits of Current Technologies in
3 Removing Per- and Polyfluoroalkyl Substances
4 from Fire Suppression Systems
5
6
7

8 AUTHORS: Dung Nguyen[1*], Christopher Bellona[2], Adria Lau[2], John Stults[1], Hayley
9   Andrews[3], David Jones[3], David Megson[3,4], Ian Ross[5]
10
11
12 AFFILIATIONS: [1]CDM Smith, 14432 SE Eastgate Way, #100, Bellevue, Washington,
13   USA
14
15   [2]Colorado School of Mines, 1500 Illinois Street, Golden, Colorado,
16   USA
17
18   [3]Manchester Metropolitan University, Chester Street, Manchester M1
19   5GD, UK
20
21   [4]Chemistry Matters, Calgary, Alberta, Canada
22
23   [5]CDM Smith, 220 Montgomery Street, #1418, San Francisco,
24   California, USA
25
26 KEY WORDS: PFAS; AFFF; decontamination; fire suppression system;
27   supramolecular assembly
28
29
30 [*]**CORRESPONDING AUTHOR**: Mailing address: CDM Smith, 14432 SE Eastgate Way,
31 #100, Bellevue, WA 98007. (425) 519-8325. Email: NguyenDD@cdmsmith.com.

32   **Abstract**

33   Several commercial products have been broadly marketed for their effectiveness in

34   removing residual PFAS from AFFF-impacted fire suppression systems. However, a

35   comprehensive assessment of their effectiveness in mitigating long-term PFAS rebound

36   following the initial cleaning has not been reported. Herein, batch and flow-through

37   experiments were conducted to interrogate the overall effectiveness of four different

38   cleaning solutions in removing residual PFAS from AFFF-impacted stainless steel pipes

39   from a fire suppression system. Advanced surface imaging techniques were also employed

40   to correlate with bench-scale testing results and to provide insights into potential PFAS

41   rebound mechanisms. Results presented herein demonstrate that complete removal of

42   PFAS from AFFF-impacted fire suppression systems is extremely difficult to achieve for

43   all four cleaning solutions examined in this study. The PFAS rebound behavior observed

44   was likely attributable to PFAS supramolecular assemblies accumulating on the pipe

45   surfaces. Because PFAS rebound following cleanout of AFFF-impacted fire suppression

46   systems is likely inevitable, there needs to be an understanding of the practical limits to

47   which impacted fire suppression system cleanout can be achieved. Improved insights into

48   the dissolution mechanisms and the rate of dissolution of supramolecular formations will

49   be key to improving PFAS decontamination processes and decontamination of

50   materials/equipment impacted by AFFFs.

51   **Environmental Implication**

52   AFFF decontamination followed by F3 transition and replacement is a critical need in

53   the United States and globally. Results from this study demonstrates that achieving

54   complete PFAS decontamination of AFFF-impacted fire suppression systems is extremely

55   difficult. PFAS supramolecular structures formed on pipe surfaces as a result of decades of

56   exposure to AFFF were consistently observed using advanced spectroscopy techniques and

57   were likely attributable to the persistent PFAS rebound behavior observed for all four

58   cleaning reagents examined in this study. Improved insights into the dissolution

59   mechanisms and the rate of dissolution of supramolecular formations will be key to

60   improving PFAS decontamination processes and decontamination of materials/equipment

61   impacted by AFFFs.

62

1. Introduction

As the United States Environmental Protection Agency (USEPA) and many states promulgate increasingly stringent regulations on acceptable concentrations of per- and polyfluoroalkyl substances (PFAS) in water and soil, pressure is rapidly increasing to replace all PFAS-containing firefighting foams such as aqueous film-forming foam (AFFF) and fluoroprotein foams historically used and stored in fire suppression systems. The National Defense Authorization Act of Fiscal Year 2020 (signed into law December 20, 2019) requires the United States Department of Defense (DoD) to immediately stop military training exercises with AFFF (Congress, 2020) and phase out its use of AFFFs at all military installations by October 1, 2024 with limited exceptions. The recent determination by the USEPA that PFAS are hazardous substances (EPA, 2024a) will likely further accelerate activities to eliminate PFAS from existing fire suppression systems and to facilitate the transition to fluorine-free foams (F3s).

In the United Kingdom and the European Union (EU), fluorinated Class B firefighting foams have been subject to assessment and may be reported as persistent organic pollutants (POPs) under the Registration, Evaluation, Authorization, and Restriction of Chemicals (REACH) regulations since 2020 (EU, 2017). All firefighting foams containing fluorosurfactants require determination of their C8 PFAS content [perfluorooctanoic acid (PFOA) and PFOA-precursors] to determine if they comprise a foam which falls under the regulatory restrictions. As part of these regulations, no training has been allowed with C8 PFAS-based foams since 2020. As of 2021, any business with more than 50 kilograms (kg) of C8 PFAS-based foam is required to register to local environmental regulators as a notifiable stockpile of POPs. Since 2023, C8 PFAS-based foams could only be used when

86   100% contained during use and the use of C8 PFAS-based foams will be terminated

87   starting in 2025. These foams of current regulatory focus have limits set on their PFOA

88   and PFOA-precursor content at 25 and 1,000 parts per billion (ppb), respectively. The total

89   oxidizable precursor (TOP) assay has been used commercially to assess the concentration

90   of C8 precursors in firefighting foams for several years (Ross, 2024). In the EU, further

91   regulations on products containing C9-C14 PFAS, with a target of 25 ppb for the sum of

92   C9-C14 perfluoroalkyl acids (PFAAs) and 260 ppb for the sum of their precursors (EU,

93   2021). In Australia, a concentration of 1 ppb of total PFAS (as confirmed by TOP assay)

94   has been stipulated as the acceptable level in the next-generation F3s (Queensland DoEaH,

95   2016 & 2017).

96   A prerequisite to the F3 transition should include thorough cleaning of AFFF-impacted

97   fire suppression systems to remove residual PFAS (API, 2020). In response to the previous

98   transition from C8- to C6-based AFFF, a triple water rinse approach was developed and

99   implemented by the United States Department of Defense (Ross, 2021; Secretary of

100   Defense for Acquisition and Sustainment, 2018) and reportedly adopted by various

101   agencies worldwide (Dahlbom et al., 2024). However, evaluation of this methodology on

102   an aircraft rescue and firefighting (ARFF) vehicle indicated that, while effective in

103   removing PFAS in AFFF from the ARFF, triple rinse with water did not reduce the

104   concentration of PFOS below 800 ppb in a subsequent rinsate sample (Edwards et al.,

105   2020). Several additional studies have highlighted the challenge of effectively removing

106   PFAS from these systems using potable water and reported substantial amount of PFAS

107   present on internal surfaces due to prolonged exposure to fluorosurfactants (Dahlbom et

108   al., 2024; Horst et al., 2021; Lang et al., 2022, Ross and Storch, 2020). The unique

109   interfacial properties of fluorosurfactants that make AFFF an effective extinguisher of

110   chemical fires have been described to form aggregates termed supramolecular assemblies

111   (Riess et al., 1996). Recent publications (Lang et al., 2022; Ross, 2021) have hypothesized

112   that this aggregation leads to formation of supramolecular assemblies of PFAS that cling

113   to the surface of fire suppression systems. These supramolecular assemblies, described by

114   Ross (2021) as a crystalline bilayer of self-assembled PFAS, are expected to be poorly

115   disrupted by water which has led to a search for more effective rinsing formulations and

116   conditions to enhance PFAS removal from impacted fire suppression systems using various

117   cosolvents or specialized cleaning agents, and/or heating, and surface scouring approaches

118   (Dahlbom et al., 2024; Edwards et al., 2020; Horst et al., 2021; Lang et al., 2022). Although

119   results from these studies indicate improved PFAS removal using the aforementioned

120   enhancements, a systematic comparison of their effectiveness is lacking.

121   Given the large number of fire suppression systems in the United States and globally

122   that have been exposed to AFFF and require cleanout, there is a critical need to

123   substantially improve the means, materials, and methods for fire suppression system

124   decontamination. Several commercial products have been recently and broadly marketed

125   for their effectiveness in removing residual PFAS from AFFF-impacted fire suppression

126   systems. However, a comprehensive assessment of their efficacy in mitigating long-term

127   PFAS rebound following the initial cleaning has not been reported. Herein, batch and flow-

128   through experiments were conducted to interrogate the overall effectiveness of four

129   different cleaning solutions in removing residual PFAS from AFFF-impacted stainless

130   steel pipes from a fire suppression system. Potentially applicable rebound mitigation

131   strategies were assessed. Advanced surface imaging techniques including high-resolution

132 scanning electron microscopy (SEM) and energy-dispersive X-ray spectroscopy (EDX)

133 were also employed to correlate with bench-scale testing results and to provide insights

134 into potential PFAS rebound mechanisms.

135 **2. Experimental Section**

136 *2.1. Materials*

137 Grade 304 stainless steel pipes measuring 7.0 cm in inner diameter and 7.6 cm in outer

138 diameter obtained from a fire suppression system at a commercial airport in Sydney,

139 Australia (courtesy of Arcadis) were used for all testing described herein. The pipes were

140 exposed to a variety of AFFF formulations for more than three decades prior to their

141 removal from the hangar. Upon receipt, the pipes were cut into small segments measuring

142 approximately 5 cm in length using a band saw. These pipe segments were then used for

143 all experiments described herein.

144 Cleaning solutions examined in this study include 1) potable water (verified to contain

145 less than 10 ng/L of total target PFAS using EPA Method 1633, see **Table SI-1**) available

146 at CDM Smith laboratory (Bellevue, WA); 2) methanol (MeOH, ACS reagent, Sigma

147 Aldrich, St. Louis, MO); 3) a solution formulated by Colorado School of Mines (Golden,

148 CO) and referred to hereafter as CSM Solution [consisting of citric acid (2% by volume),

149 ethanol (10%), propylene glycol (20%), and potable water (68%); all chemicals purchased

150 from Sigma Aldrich, St. Louis, MO]; and 4) and a proprietary, commercial cleaning

151 solution widely used for AFFF cleanout from impacted fire suppression systems, which is

152 composed of a biodegradable, plant-based fatty acid that forms a weak ionic bond with

153 anionic PFAS constituents (referred to hereafter as Proprietary Solution). Potable water

154 was chosen to serve as a negative control in this study whereas methanol, given its high

155 solvency for PFAS, was used as a positive control. The Proprietary Solution was included

156 in this study because it is one of the few reagents currently marketed for fire suppression

157 system cleaning. The CSM Solution, consisting of citric acid, ethanol, and propylene glycol,

158 was specifically formulated for field demonstration due to its lowered pH and inclusion of

159 solvents with low flammability and high solvency for PFAS.

160 *2.2. Batch Experiments*

161   5-cm long segments of the AFFF-impacted pipes were placed in 4-L HDPE containers

162 pre-cleaned with methanol and PFAS-free DI water (**Figure SI-1**). The four cleaning

163 solutions examined were then added to the HDPE containers to completely submerge the

164 pipes. The capped HDPE containers were then placed in a temperature-controlled (20 $^{\circ}$C)

165 shaker table and agitated at 80 rpm for 24 hours. After the 24-hour period, an aqueous

166 sample was collected from each HDPE container for target and non-target PFAS analysis

167 (described below). Subsequently, the PFAS-laden "spent" cleaning solution was

168 completely removed from each HDPE container and replaced with a fresh solution. This

169 solution changeout process was repeated three times to simulate the triple rinse protocol

170 commonly employed for fire suppression system cleanout. At the end of the triple rinse,

171 PFAS-free DI water was then added into the HDPE containers to simulate the F3

172 replacement in the "clean" fire suppression system that typically occurs following AFFF

173 cleanout. Due to the difficulty in analyzing for PFAS samples in F3, PFAS rebound was

174 evaluated in DI water instead of a F3. The HDPE containers were then agitated in the

175 shaker table for an additional 2-, 4-, and 6-weeks with samples collected at each interval

176 (to simulate and to assess the potential for post-cleaning PFAS rebound). Following

177 collection of the 6-week rebound test, the pipes were rinsed with methanol. Subsequently,

178   samples of the methanol rinsates were collected to determine the extent of residual PFAS

179   remaining on the surfaces of the pipes. All testing was performed in duplicate to assess

180   data reproducibility.

181   *2.3. Surface Agitation Techniques*

182   Two different surface agitation techniques were interrogated for their potential

183   effectiveness in mitigating PFAS rebound following the triple rinse. Testing was performed

184   using the same AFFF-impacted pipe segments and the aforementioned batch testing

185   protocols with the exception that, following the triple rinse, the impacted pipes were subject

186   to either physical scrubbing using a 5.7-cm diameter, hard-bristled, stainless steel brush

187   (Fisher Scientific, Waltham, MA) connected with a power drill for 1 hour or ultrasonic

188   cleaning in methanol for approximately 15 days using an ultrasonic cleaner (VWR

189   Aquasonic Model 150T, 35 kHz). Subsequently, the pipes were soaked in PFAS-free DI

190   water and subject to rebound evaluation at 2-, 4-, and 6-weeks following the initial cleaning

191   as previously described. Additional experiments were performed on DI water spiked with

192   a C6 AFFF (Phos-Chek 3% AFFF MilSpec, Asturias, Spain) to ensure no PFAS

193   degradation occurred via sonolysis as a result of sonication; this is consistent with literature

194   results which reported little to no PFAS degradation at a frequency of 44 kHz or lower

195   (Wood et al., 2020).

196   *2.4. Flow-Through Experiments*

197   To more realistically simulate AFFF cleanout from impacted fire suppression systems

198   under field conditions (where continuous recirculation of a cleaning solution is typically

199   performed during AFFF cleanout) and to ensure that results obtained from the

200   aforementioned batch experiments were not an artifact of the batch testing methodology,

201 flow-through experiments were performed utilizing the same AFFF-impacted pipes and

202 three cleaning reagents including potable water, the CSM Solution, and the Proprietary

203 Solution (**Figure SI-2**). For safety reasons, methanol was not examined in these flow-

204 through experiments. A 4-L glass media bottle was used as the reservoir for the cleaning

205 solution. A centrifugal pump was used to recirculate the cleaning solution through the

206 AFFF-impacted pipes in an up-flow configuration. Aqueous samples were periodically

207 collected from the reservoir to assess PFAS removal effectiveness from the impacted pipes.

208 Similar to the batch experiments, the triple rinse protocol was simulated in these flow-

209 through experiments; after each 8-hour continuous recirculation event, a "fresh" cleaning

210 solution was used to replace the "spent" PFAS-laden solution. After the third rinse, the

211 pipes were transferred to pre-cleaned 4-L HDPE containers and allowed to soak in PFAS-

212 free DI water to assess post-cleaning PFAS rebound as previously described; again, the

213 intent herein was to simulate the potential PFAS rebound in the replacement F3 in fire

214 suppression systems following AFFF cleanout. Similar to the batch experiments, rebound

215 testing was performed in DI water instead of a F3 due to analytical interreferences. Note

216 that PFAS rebound mitigation strategies employed in the batch experiments including

217 physical scrubbing and sonication in methanol are difficult (if not impossible) to implement

218 in the field. Therefore, air scouring, a commonly employed surface scouring method, and

219 mild heating (50 °C) were evaluated as potential PFAS rebound mitigation strategies in

220 these flow-through experiments. Other surface scouring techniques such as sand blasting

221 and utilization of solid-phased scouring agents were deemed unacceptable to the DoD fire

222 suppression system operators and thus were not evaluated as part of this study. An air

223 compressor was used to introduce air into the continuous recirculation loop at

224 approximately 2 L/min to assess impacts of scouring on PFAS removal from impacted pipe

225 surfaces and post-cleaning PFAS rebound potential. To evaluate impacts of mild heating,

226 separate experiments were performed for all three solutions examined in the flow-through

227 experiments at ambient (approximately 22 $^{\circ}$C) as well as an elevated temperature

228 (approximately 50 $^{\circ}$C). A hot plate was used to increase the temperature of the recirculating

229 cleaning solution to the desired temperature. All testing was performed in duplicate to

230 assess data reproducibility.

231 *2.5. Total Extractable PFAS Mass Determination*

232   Triplicate pipe segments were subject to long-term ultrasonic cleaning in methanol to

233 determine the total extractable mass of PFAS present on pipe surfaces. The same ultrasonic

234 cleaning procedure used in the previously described surface agitation experiments was

235 employed, with the exception that the methanol rinsate solution was analyzed for pre- and

236 post-oxidation PFAS and replaced each day for a total of 15 days until PFAS were no

237 longer detected in the rinsate. The PFAS mass extracted from each ultrasonic cleaning

238 cycle was subsequently added to determine the total extractable PFAS mass from the

239 AFFF-impacted pipe surfaces.

240 *2.6. PFAS Analyses*

241   All PFAS analyses were performed using liquid chromatography with tandem mass

242 spectrometry (LC-MS/MS) by SGS-AXYS Analytical (British Columbia, Canada) via

243 EPA Method 1633 (EPA, 2024b). The reporting limits for all 40 target PFAS were

244 approximately 1 ng/L. TOP assay samples were also analyzed in the same manner, with

245 the exception that samples were subject to heat- and alkaline-activated persulfate oxidation

246 to transform perfluoroalkyl acid (PFAA) precursors to terminal PFAAs prior to the routine

247   target PFAS analysis using EPA Method 1633. All TOP assay samples were also conducted

248   by SGS-AXYS Analytical. The reporting limits for all PFAS in TOP assay following

249   oxidation were more elevated than the pre-oxidation analysis, ranging between

250   approximately 5 and 20 ng/L.

251   *2.7. Surface Imaging*

252   Pipe samples exhibiting PFAS rebound (following triple rinse with methanol) and those

253   exhibiting little rebound post-cleaning (following ultrasonic cleaning in methanol) in the

254   batch experiments were sent to Manchester Metropolitan University for surface imaging

255   using SEM and EDX techniques. All pipe samples were cut into pieces measuring

256   approximately 2 cm x 2 cm in size using a hacksaw. The samples were then mounted on

257   the aluminum SEM pin stubs (12 mm diameter, Agar Scientific, Essex, UK) using adhesive

258   carbon tabs (12 mm diameter, Agar Scientific, Essex, UK). Subsequently, the samples were

259   loaded into a Crossbeam 350 Focused Ion Beam – Scanning Electron Microscope (FIB-

260   SEM) (Carl Zeiss GmbH, Oberkochen, Germany) fitted with a field emission electron gun.

261   Backscattered electron images were obtained using an Energy-Selective Backscattered

262   Electron (EsB) detector using an accelerating voltage of 2 kV and the filtering grid set to

263   1.5 kV to remove the secondary electron signal. With SEM, backscattered electrons arise

264   as a result of elastic scattering of incident beam electrons by atoms on the sample surface

265   (Marassi at al., 2009). Due to their larger nuclei, heavier elements can deflect the incident

266   electrons through larger angles, meaning that they are more likely to escape from the

267   sample surface and be subsequently detected. Therefore, materials with higher atomic

268   numbers will generate more backscattered electrons than materials with a low atomic

269   number. With EDX, the X-rays generated as a result of inelastic collisions of incident beam

270   electrons with various atoms on the sample surface can be measured by an EDX detector

271   and used to determine the elemental composition of the analyzed area. EDX analysis was

272   performed using an Ultim Max 170 detector (Oxford Instruments plc., Abingdon, UK).

273   EDX spectra were obtained from several areas across each sample at low magnification

274   using an accelerating voltage of 20 kV.

275   **3. Results and Discussion**

276   *3.1. Batch Experiment Results*

277   The total target PFAS mass (dominated by 6:2 FTS as shown in **Figure SI-3**) removed

278   by the four cleaning reagents (expressed as PFAS mass removed normalized by the inner

279   surface area of the pipes exposed to AFFF or ng/cm^2) after the initial triple rinse followed

280   by the 2-, 4-, and 6-week rebound periods in PFAS-free DI water, and after the final

281   methanol rinse is depicted below in **Figure 1A**. A summary of the total PFAS masses

282   recovered during the initial triple rinse as well as in the four subsequent rebound samples,

283   normalized by the inner pipe surface area, is tabulated in **Table 1**. The corresponding PFAS

284   concentrations of the rinsate and rebound (in DI water) samples are presented in **Table SI-**

285   **2**. For all four cleaning solutions examined in this study, the highest PFAS masses

286   recovered in the rinsates were observed following the initial rinse. The surface-normalized

287   pre-oxidation PFAS masses recovered during the initial rinse were approximately 120, 170,

288   250, and 290 ng/cm^2 for the Proprietary Solution, potable water, methanol, and CSM

289   Solution, respectively. The pre-oxidation PFAS mass recovered from the pipes decreased

290   significantly after the initial triple rinse, subsequently rebounded over the 6-week periods

291   of soaking in DI water, and increased even further after the final methanol rinse. However,

292   the extent to which PFAS rinsate concentrations decreased initially and subsequently

293 rebounded varied among the four cleaning solutions examined. Specifically, the highest

294 pre-oxidation PFAS masses were recovered following the triple rinse with methanol

295 (approximately 270 ng/cm^2) and the CSM solution (approximately 300 ng/cm^2).

296 Additionally, the least amount of target PFAS mass was recovered in the third rinse using

297 were attained using methanol and the CSM Solution (approximately 1 ng/cm^2). The

298 smallest extent of PFAS rebound over the 6-week period after the initial cleanout and

299 following the final methanol rinse were also observed using methanol and the CSM

300 Solution (measured approximately 110 and 60 ng/cm^2 total in the four rebound samples

301 collected after the initial triple rinse, respectively). In several cases, the CSM Solution

302 statistically outperformed methanol (with a 95% confidence), albeit only slightly. On the

303 other hand, both potable water and the Proprietary Solution were generally the least

304 effective solutions with respect to maximizing PFAS removal from impacted pipes after

305 the triple rinse while minimizing PFAS rebound in the subsequent rebound and methanol

306 rinse samples. Specifically, only approximately 160 and 220 ng/cm^2 of target PFAS masses

307 were recovered after the initial triple rinse using the Proprietary Solution and potable water,

308 respectively. Substantially higher residual PFAS masses were observed in the third rinse

309 using the Proprietary Solution (approximately 17 ng/cm^2) and potable water

310 (approximately 25 ng/cm^2) compared to methanol and the CSM solution (approximately 1

311 ng/cm^2). A higher degree of PFAS rebound following the initial triple rinse was observed

312 with the Proprietary Solution and potable water compared to methanol and the CSM

313 solution (with a 95% confidence). The PFAS masses recovered in the final methanol rinse

314 samples represented between 70 and 130% of those observed after the first rinse using

315 potable water and the Proprietary Solution, respectively. Surprisingly, the Proprietary

316 Solution was even less effective than potable water. In fact, lower PFAS removal and

317 higher PFAS rebound were observed with the Proprietary Solution compared to potable

318 water. As provided in **Table SI-2**, very high target PFAS aqueous concentrations were

319 observed in the 6-week rebound samples in DI water, ranging from approximately 3,000,

320 7,000, 10,500, and 11,200 ng/L for the CSM Solution, methanol, potable water, and the

321 Proprietary Solution, respectively. These very high pre-oxidation PFAS concentrations in

322 the DI water-based rebound samples are noteworthy given the requisite residual PFAS

323 concentration threshold of less than 1 ppb for the next-generation F3s (DoD, 2023) and

324 EPA's recent PFAS rule (EPA, 2024c).

325   Substantially higher (between approximately 15 and 20 times) PFAS concentrations

326 were observed following the TOP assay as shown in **Figure 1B**, suggesting that there is a

327 significant amount of PFAA precursors present in the rinsates that were readily oxidized

328 to terminal PFAAs. Interestingly, similar PFAS removal and rebound trends were observed

329 for pre- and post-oxidation results. In general, the CSM Solutions and methanol were the

330 most effective cleaning reagents; the highest PFAS concentrations in the rinsates and the

331 smallest extent of PFAS rebound were observed with these solutions. The post-oxidation

332 aqueous PFAS concentrations present in the 6-week rebound samples (in DI water)

333 following the initial triple rinse ranged from approximately 46,000, 53,000, 103,000 to

334 126,000 ng/L for the CSM Solution, methanol, potable water, and the Proprietary Solution,

335 respectively. These concentrations are several orders-of-magnitude higher than the

336 aforementioned performance specification for the next-generation F3s.
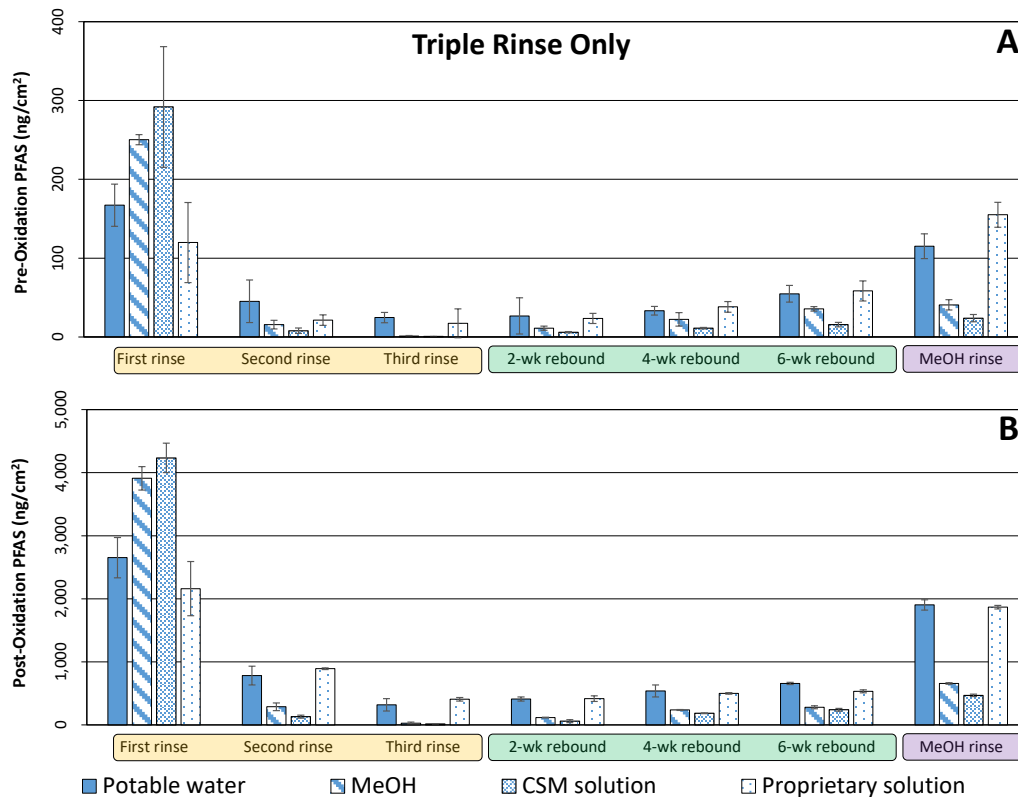
Figure 1. Total Pre-Oxidation (A) and Post-Oxidation (B) PFAS Mass Removed from AFFF-Impacted Pipes Using Triple Rinse with Different Cleaning Solutions
Average results shown. Error bars = 95% confidence interval. PFAS masses recovered in the rinsate were normalized by the inner surface area of the pipes exposed to AFFF (i.e., ng PFAS per cm^2).

Impacts of pipe surface agitation on minimizing PFAS rebound following the initial triple rinse using physical scrubbing and ultrasonic cleaning techniques are graphically illustrated below in **Figures 2** and **3**, respectively. In general, ultrasonic cleaning in methanol was slightly more effective than physical scrubbing in mitigating the PFAS rebound potential; more than 98% reduction of both total pre- and post-oxidation PFAS concentrations were observed and sustained following the initial triple rinse coupled with ultrasonic cleaning in methanol. With surface agitation, substantially lower PFAS aqueous concentrations were observed in the 6-week rebound samples for all four cleaning solutions examined, ranging between approximately 10 and 200 ng/L. Interestingly, there were little

differences (with a 95% confidence) in the extent to which PFAS rebound were mitigated among the four cleaning solutions examined in this study after either pipe surface agitation technique had been applied. These results suggest that pipe surface agitation may be more influential in limiting potential PFAS rebound following the initial triple rinse than the actual cleaning solution employed. An alternative set of data charts, plotted in logarithmic scale to better visualize differences across the cleaning reagents at lower concentrations, is provided in **Figure SI-4**.
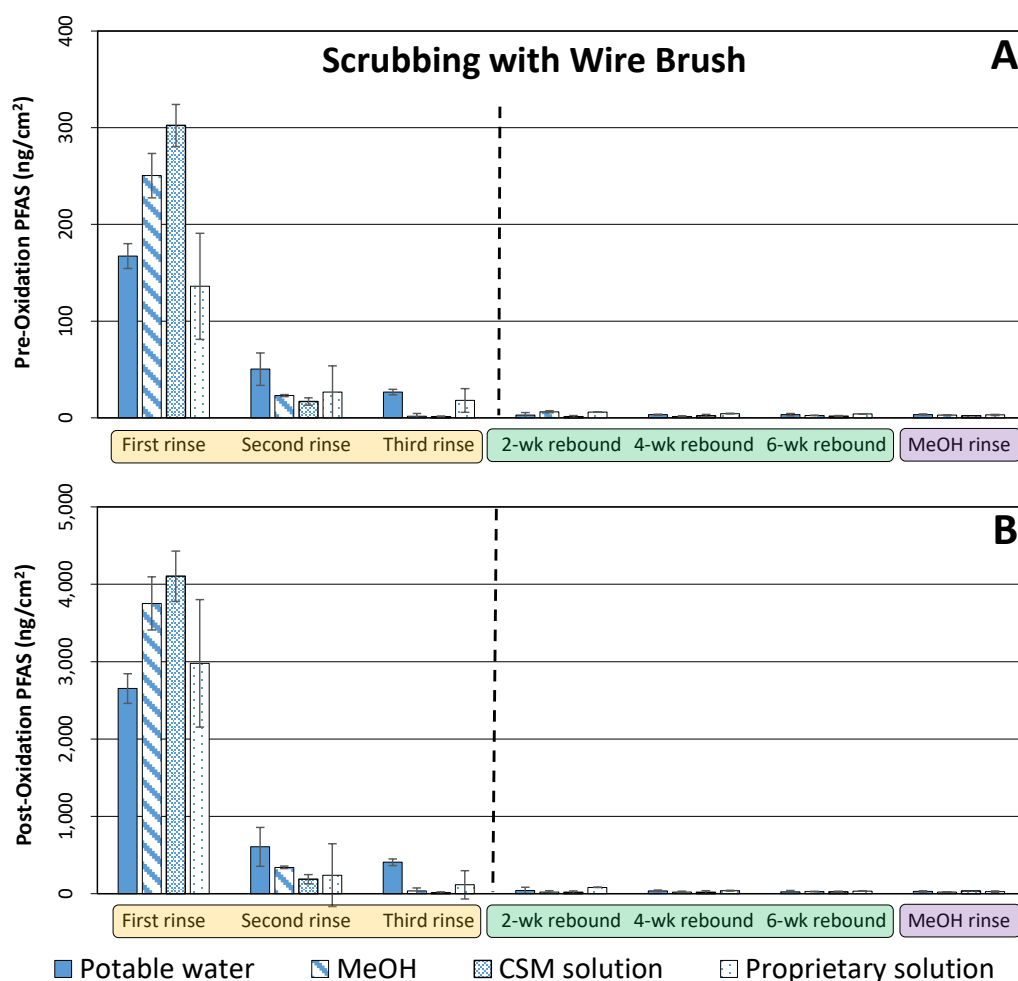
Figure 2. Total Pre-Oxidation (A) and Post-Oxidation (B) PFAS Mass Removed from AFFF-Impacted Pipes Using Different Cleaning Solutions with Physical Scrubbing
Average results shown. Error bars = 95% confidence interval. PFAS masses recovered in the rinsate were normalized by the inner surface area of the pipes exposed to AFFF (i.e.,

ng PFAS per cm²). Dashed line represents when physical scrubbing using a hard-bristled brush was performed following the initial triple rinse.

367
368
369
370
371
372
373
374

375

376

377

378

379
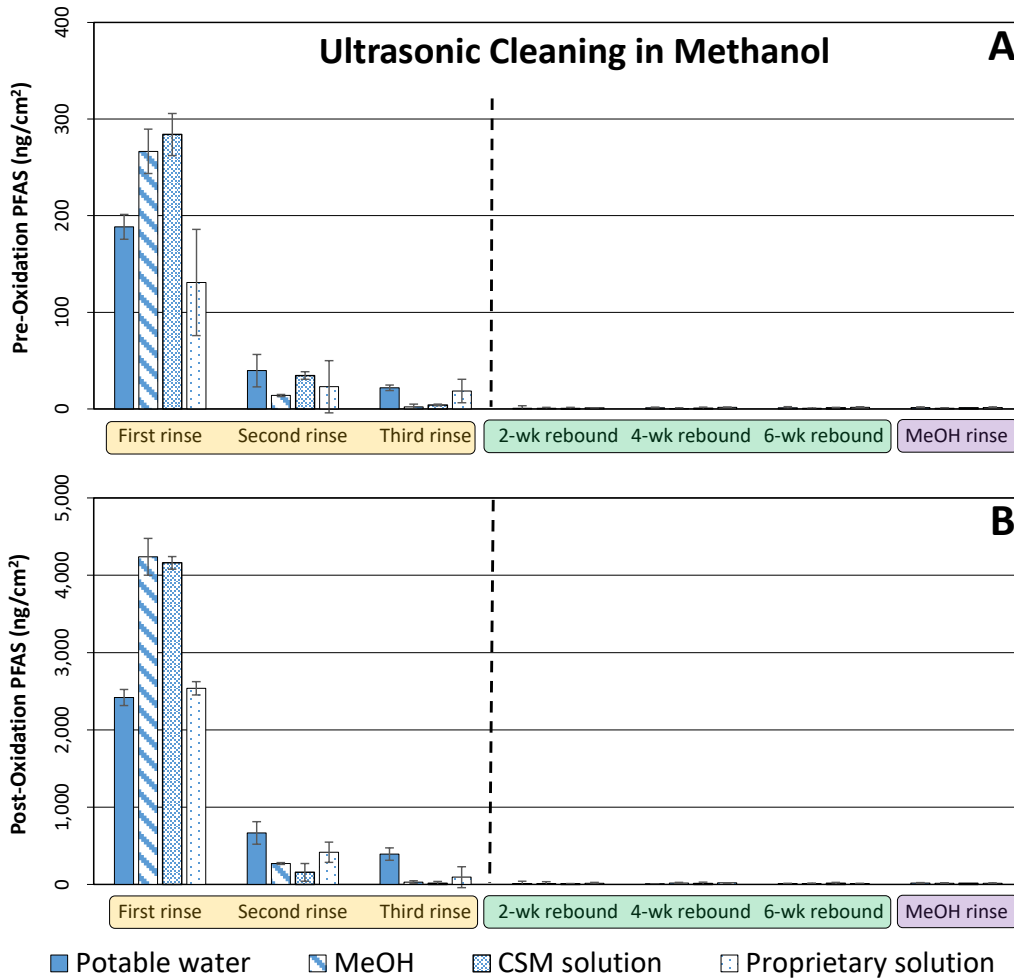
Figure 3. Total Pre-Oxidation (A) and Post-Oxidation (B) PFAS Mass Removed from AFFF-Impacted Pipes Using Different Cleaning Solutions with Ultrasonic Cleaning *Average results shown. Error bars = 95% confidence interval. PFAS masses recovered in the rinsate were normalized by the inner surface area of the pipes exposed to AFFF (i.e., ng PFAS per cm²). Dashed line represents when ultrasonic cleaning was performed following the initial triple rinse.*

Table 1. Total Surface Area-Normalized PFAS Mass Removed Pre- vs. Post-Oxidation During the Initial Triple Rinse and Subsequent Rebound Tests in the Batch Experiments

Surface agitation techniques	Cleaning solution	PFAS concentration (ng/cm^2)			
		Pre-oxidation		*Post-oxidation*	
		Triple rinse	Rebound	Triple rinse	Rebound
None	Potable water	240 ± 15	230 ± 6	3,800 ± 240	3,500 ± 210
	MeOH	270 ± 10	110 ± 16	4,200 ± 150	1,200 ± 150
	CSM solution	300 ± 11	60 ± 4	4,400 ± 320	850 ± 100
	Proprietary solution	160 ± 21	280 ± 11	3,500 ± 430	3,300 ± 160
Scrubbing with wire brush after triple rinse	Potable water	240 ± 16	13 ± 2	3,700 ± 170	130 ± 14
	MeOH	280 ± 14	17 ± 1	4,100 ± 250	90 ± 10
	CSM solution	320 ± 18	7 ± 2	4,300 ± 310	100 ± 15
	Proprietary solution	180 ± 26	13 ± 1	3,300 ± 30	182 ± 20
Ultrasonic cleaning in methanol after triple rinse	Potable water	250 ± 13	4 ± 1	3,500 ± 200	50 ± 10
	MeOH	280 ± 11	4 ± 1	4,500 ± 140	60 ± 11
	CSM solution	320 ± 26	4 ± 1	4,300 ± 200	50 ± 9
	Proprietary solution	170 ± 28	6 ± 1	3,100 ± 320	70 ± 11

Masses recovered from the initial triple rinse are sums of those measured following the first, second, and third rinses with each of the four cleaning solutions examined. Masses recovered from rebound testing are sums of those measured in the 2-, 4-, and 6-weeks post-cleaning rebound samples as well as in the final methanol rinses.

3.2. Flow-Through Experiment Results

Results of the flow-through experiments for the three solutions examined (methanol was not interrogated due to safety reasons) are graphically depicted in **Figure 4**. The similarity (±10%) in PFAS masses removed and those rebounded between the flow-through and the batch experiments indicated that the results observed in the batch experiments were not an artifact of the experimental setup. Additionally, these results demonstrated that continuous recirculation of the cleaning reagents through the impacted pipes alone do not meaningfully improve AFFF cleanout effectiveness. Impacts of surface agitation techniques that can be readily applied at the field scale, including air scouring and mild heating, on enhancing PFAS removal from impacted pipe surfaces and minimizing PFAS rebound following the initial triple rinse are shown in **Figures 4A** and **4B**, respectively. For ease of comparison, only relative changes in PFAS mass recovered following the initial triple rinses (representative of the readily PFAS removal) and in

400 subsequent rebound samples in PFAS-free DI water (representative of the PFAS rebound

401 potential) are presented herein and tabulated in **Table 2**. Little to no improvements were

402 seen with air scouring for all three cleaning solutions examined, suggesting that more

403 aggressive surface agitation techniques are likely required to meaningfully enhance PFAS

404 removal and to minimize potential for PFAS rebound. Mild heating to 50 $^{\circ}$C marginally

405 improved PFAS removal (by up to 40%) from impacted pipe surfaces and mitigated

406 potential PFAS rebound (by up to 30%) following the triple rinse for all three solutions

407 examined except for the Proprietary Solution [where only a marginal (approximately 20%)

408 improvement in PFAS removal and rebound mitigation was observed]. Duplicate

409 measurements were taken in an attempt to account for analytical errors and variability in

410 PFAS concentration across the pipe length. However, it is recognized that some of the

411 discrepancy might be attributable to variations in the different pipe segments used

412 throughout the experiments and/or within analytical errors. Collectively, these results

413 suggest that mild heating coupled with a more aggressive surface agitation technique

414 should be considered to optimize PFAS removal from impacted pipe surfaces and to

415 minimize PFAS rebound.

416
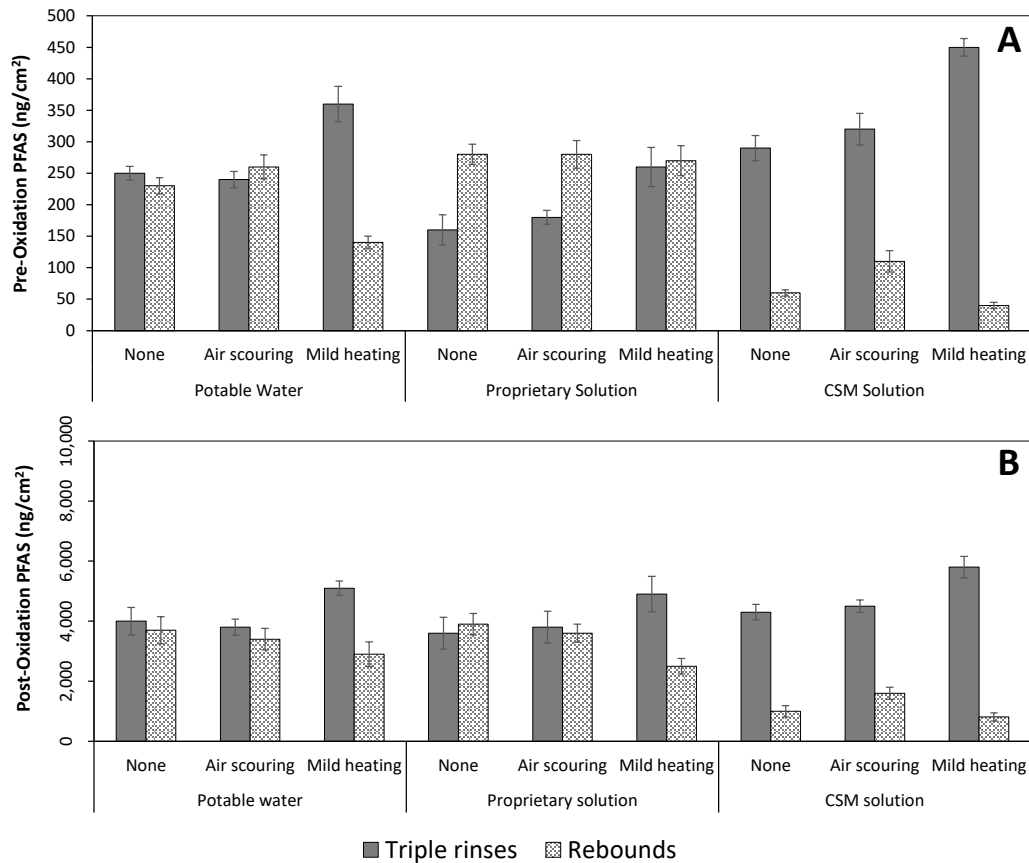
417
418 **Figure 4.** Impacts of Air Scouring and Mild Heating on Pre-Oxidation (A) and Post-
419 Oxidation (B) PFAS Removal and PFAS Rebound Potential in the Flow-Through
420 Experiments
421 *Average results shown. Error bars = 95% confidence interval. PFAS concentrations in the*
422 *rinsate were normalized by the inner surface area of the pipes exposed to AFFF. Masses*
423 *recovered from the triple rinses are sums of those measured following the first, second,*
424 *and third rinses with each of the three cleaning solutions examined. Masses recovered from*
425 *rebound testing are sums of those measured in the 2-, 4-, and 6-weeks post-cleaning*
426 *rebound samples as well as in the final methanol rinses. Except for the mild heating*
427 *experiments (which were conducted at approximately 50 ℃), all other experiments were*
428 *conducted at ambient temperature of approximately 22 ℃.*
429
430
431
432
433
434
435
436
437
438

439 **Table 2**. Total Surface Area-Normalized PFAS Mass Removed Pre- vs. Post-Oxidation
440 During the Initial Triple Rinse and Subsequent Rebound Tests in the Flow-Through
441 Experiments

Surface agitation techniques	Cleaning solution	PFAS concentration (ng/cm^2)			
		Pre-oxidation		Post-oxidation	
		Triple rinse	Rebound	Triple rinse	Rebound
None	Potable water	250 ± 11	230 ± 13	4,000 ± 460	3,700 ± 450
	CSM solution	290 ± 20	60 ± 5	4,300 ± 260	1,000 ± 190
	Proprietary solution	160 ± 24	280 ± 16	3,600 ± 530	3,900 ± 360
Air scouring	Potable water	240 ± 13	260 ± 19	3,800 ± 270	3,400 ± 360
	CSM solution	320 ± 25	110 ± 17	4,500 ± 210	1,600 ± 200
	Proprietary solution	180 ± 11	280 ± 22	3,800 ± 530	3,600 ± 300
Mild heating	Potable water	360 ± 28	140 ± 10	5,100 ± 240	2,900 ± 410
	CSM solution	450 ± 14	40 ± 5	5,800 ± 360	810 ± 140
	Proprietary solution	240 ± 31	270 ± 24	4,900 ± 590	2,500 ± 260

442 *Masses recovered from the initial triple rinse are sums of those measured following the*
443 *first, second, and third rinses with each of the four cleaning solutions examined. Masses*
444 *recovered from rebound testing are the sums of those measured in the 2-, 4-, and 6-weeks*
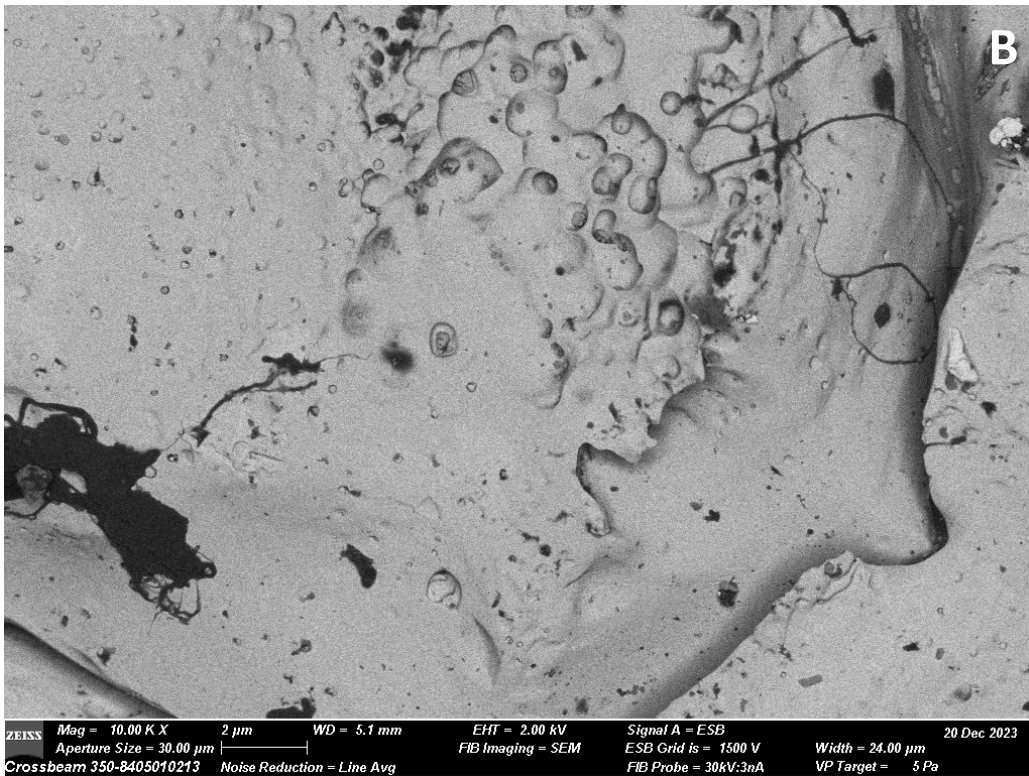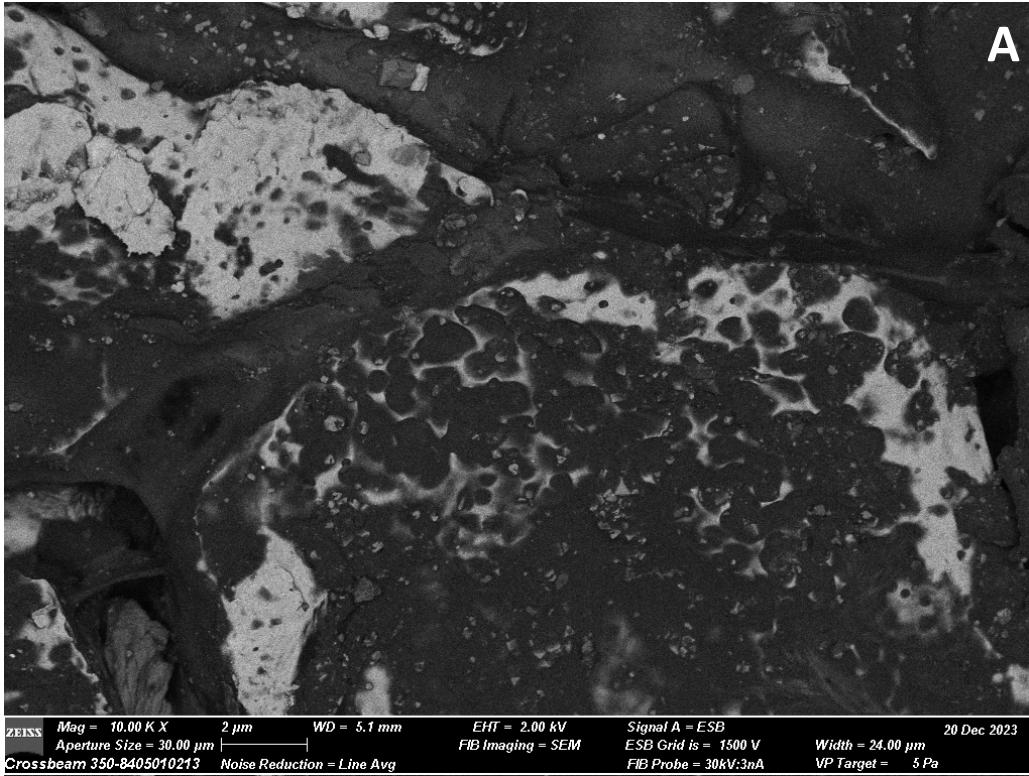445 *post-cleaning rebound samples as well as in the final methanol rinses.*
446
447   When compared to the total PFAS mass that can be extracted from the impacted pipes

448 (approximately 1,400 ng/cm^2 pre-oxidation or 16,000 ng/cm^2 post-oxidation as shown in

449 **Table SI-3**), the maximum PFAS mass recovered in the flow-through experiments

450 following the initial triple rinse with the CSM solution and mild heating only represented

451 less than half of the total extractable PFAS mass present on pipe surfaces. These results

452 highlight the challenge in completely removing PFAS from AFFF-impacted fire

453 suppression systems while minimizing post-cleaning PFAS rebounds.

454 *3.3. Pipe Surface Imaging Results*

455   SEM images of pipes exhibiting significant (triple rinse with methanol as shown in

456 **Figure 1**) and minimal (ultrasonic cleaning in methanol as shown in **Figure 3**) PFAS

457 rebound are shown in **Figures 5A** and **5B**, respectively. There is a significant difference in

458 the contrast of the backscattered electron images obtained from the two pipe samples. In

459 the "dirty" pipe sample subject to triple rinse with methanol (which exhibited significant

460 PFAS rebound), the majority of the pipe surface is covered by dark patches indicative of

461   low atomic number (i.e., lighter) elements. In contrast, in the "clean" pipe sample subject

462   to ultrasonic cleaning in methanol (which exhibited substantially less PFAS rebound), there

463   is a significant reduction in the coverage of the dark patches and substantially more lighter

464   patches which are indicative of high atomic number (i.e., heavier) elements.

465

Panel A (top):
ZEISS | Mag = 10.00 K X | 2 µm | WD = 5.1 mm | EHT = 2.00 kV | Signal A = ESB | 20 Dec 2023
Aperture Size = 30.00 µm | FIB Imaging = SEM | ESB Grid is = 1500 V | Width = 24.00 µm
Crossbeam 350-8405010213 | Noise Reduction = Line Avg | FIB Probe = 30kV:3nA | VP Target = 5 Pa

Panel B (bottom):
ZEISS | Mag = 10.00 K X | 2 µm | WD = 5.1 mm | EHT = 2.00 kV | Signal A = ESB | 20 Dec 2023
Aperture Size = 30.00 µm | FIB Imaging = SEM | ESB Grid is = 1500 V | Width = 24.00 µm
Crossbeam 350-8405010213 | Noise Reduction = Line Avg | FIB Probe = 30kV:3nA | VP Target = 5 Pa

Figure 5. SEM Images of "Dirty" Pipes Exhibiting Significant (A) Versus "Clean" Pipes Exhibiting Little (B) Post-Cleaning PFAS Rebound

10,000x magnification. Darker patches = lighter elements. Lighter patches = heavier elements.

471   Further pipe surface analysis was performed using EDX to determine the elemental

472   composition of the analyzed area. The EDX quantification data, tabulated below in **Table**

473   **3** and depicted in **Figure 6,** shows substantially higher amount of carbon, oxygen, and

474   fluorine on the "dirty" pipe surfaces (**Figure 6A**) than on the "clean" pipe surfaces (**Figure**

475   **6B**), which is consistent with observations made with the backscattered electron images

476   (**Figure 5**). The average mass of fluorine detected in the "dirty" pipe samples is

477   approximately 1.0% (by weight). No fluorine was detected in any of the three areas

478   analyzed on the "clean" pipe. In addition to fluorine, higher average masses of carbon (15%

479   vs. 10%) and oxygen (3% vs. 1%) were consistently observed on the "dirty" pipe surfaces

480   than on the "clean" pipe surfaces, thereby serving as indirect evidence of fluorosurfactant

481   supramolecular assemblies on the "dirty" pipes. In contract, higher masses of chromium,

482   iron, and nickel (the three most abundant elements found in Grade 304 stainless steel) were

483   observed on the surfaces of the "clean" pipe samples (**Figures 5B** and **6B**) with little to no

484   coating consisting of carbon, fluorine, and oxygen.

485   **Table 3**. EDX Elemental Analysis (% by Weight) of "Dirty" vs. "Clean" Pipe Surfaces

Element	Dirty pipe 1	Dirty pipe 2	Dirty pipe 3	Clean pipe 1	Clean pipe 2	Clean pipe 3
C	18.0 ± 6.1	15.6 ± 5.9	11.6 ± 11.2	10.3 ± 4.4	8.6 ± 1.0	12.8 ± 0.8
O	4.3 ± 3.2	3.0 ± 2.4	2.6 ± 1.9	1.0 ± 0.0	1.0 ± 0.1	1.7 ± 0.2
F	1.3 ± 0.6	1.0 ± 0.3	1.2 ± 0.0	-	-	-
Na	1.0 ± 0.1	0.8 ± 0.5	0.7 ± 0.2	-	-	-
Al	0.3 ± 0.3	0.4 ± 0.1	0.2 ± 0.0	-	-	0.2 ± 0.0
Si	0.3 ± 0.1	0.2 ± 0.1	0.3 ± 0.1	0.3 ± 0.1	0.4 ± 0.0	0.4 ± 0.1
S	0.6 ± 0.4	0.5 ± 0.4	0.2 ± 0.0	0.1 ± 0.0	-	0.1 ± 0.0
Cl	0.2 ± 0.1	0.2 ± 0.2	0.1 ± 0.0	-	-	-
K	0.2 ± 0.0	-	0.1 ± 0.0	-	-	-
Ca	0.1 ± 0.0	0.2 ± 0.1	0.1 ± 0.0	-	-	0.2 ± 0.0
Ti	0.1 ± 0.0	-	-	-	-	0.2 ± 0.1
V	0.1 ± 0.0	-	-	0.1 ± 0.0	-	-
Cr	14.8 ± 1.5	16.8 ± 2.9	16.8 ± 2.5	17.6 ± 0.9	17.7 ± 0.5	16.8 ± 0.2
Mn	0.8 ± 0.1	1.2 ± 0.3	1.1 ± 0.3	0.9 ± 0.1	1.0 ± 0.1	0.9 ± 0.1
Fe	52.5 ± 7.3	55.1 ± 5.6	58.0 ± 7.4	63.6 ± 2.4	64.2 ± 1.2	60.6 ± 1.1
Ni	5.7 ± 0.8	5.3 ± 1.9	6.2 ± 0.3	6.8 ± 0.8	7.4 ± 0.4	7.2 ± 0.4
Cu	-	-	-	-	0.3 ± 0.0	-

Element	Dirty pipe 1	Dirty pipe 2	Dirty pipe 3	Clean pipe 1	Clean pipe 2	Clean pipe 3
Zn	-	0.7 ± 0.0	-	-	-	-

All elemental masses reported as % by weight. Average results of triplicate analyses shown with 95% confidence intervals.
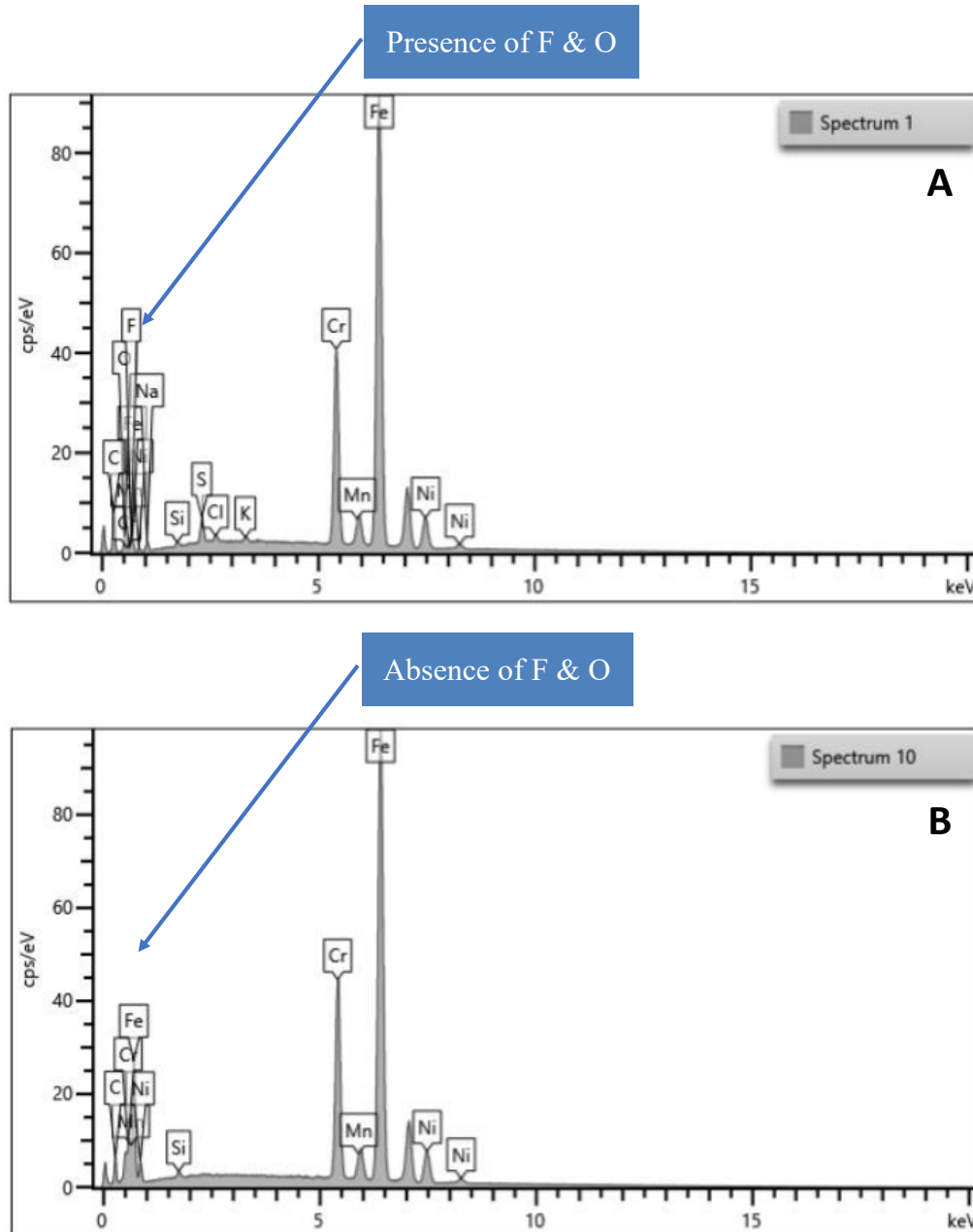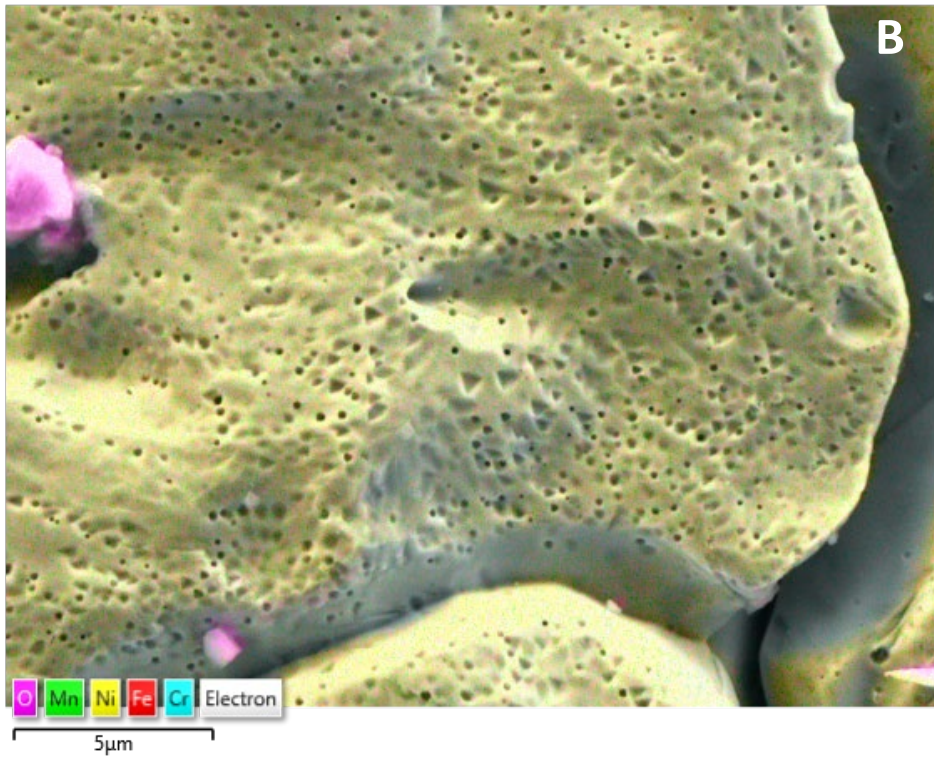

Figure 6. EDX Images of "Dirty" Pipes Exhibiting Significant (A) Versus "Clean" Pipes Exhibiting Little (B) Post-Cleaning PFAS Rebound

495   High-resolution EDX maps of the "dirty" pipes exhibiting significant PFAS rebound

496   versus "clean" pipes exhibiting little post-cleaning PFAS rebound are shown in **Figures**

497   **7A** and **7B**, respectively. No fluorine was found on the surfaces of the "clean" pipes,

498   consistent with the bench testing results and EDX images presented above. On the other

499   hand, high-resolution EDX maps for fluorine only (shown in **Figure SI-5**) suggest that the

500   PFAS was uniformly distributed across the entire surface of the impacted pipe like a

501   coating; these results are also consistent with the bench testing results and EDX images

502   presented above. Note that the majority of green masses seen across the surface of the

503   AFFF-impacted pipes in **Figure 7A** contained little fluorine (see **Figure SI-5**) and are

504   likely associated with the carbon and oxygen present on the pipe surface. A small amount

505   of fluorine is present in select green masses. Recent experimental and historical evidence

506   has demonstrated that PFAS can form supramolecular structures on the surface of solid or

507   hydrophobic materials (Kraft et al., 2009; Kostarelos et al., 2020; Dong et al., 2021;

508   Tsianou et al., 2023; Mohona et al., 2023). In one study, microemulsions large enough to

509   clog the pore space were formed by AFFF and non-aqueous phase liquids (NAPLs)

510   (Kostarelos et al., 2020). Based on these characteristics, it is possible that the large amounts

511   of fluorine mass in the surface defects of the pipe are supramolecular PFAS structures. The

512   surface defects may represent diffusion limited transport domains and the supramolecular

513   PFAS structures in those domains may be analogous to residual NAPLs trapped within

514   tightly held layers (Miller et al., 1990; Powers et al., 1994a; Powers et al., 1994b). These

515   structures may be directly responsible for the ongoing PFAS rebound observed following

516   the initial triple rinse in both the batch and flow-through experiments. This is an active area

517   of reach and warrants further evaluation using other imaging techniques such as X-ray

518   photoelectron spectroscopy (XPS), Fourier-transform infrared (FTIR) spectroscopy, and

519   Raman spectroscopy.

520

Figure 7. High-Resolution EDX Images of "Dirty" Pipes with Fluorine-Containing Materials (A) Versus "Clean" Pipes Exhibiting No Fluorine-Containing Material (B)

4. Conclusions

Results presented herein demonstrate that complete removal of PFAS from AFFF-impacted fire suppression system is extremely difficult, even in the "best-case scenario" addressing straight pieces of stainless-steel pipe at the bench scale and using PFAS-free DI water in the rebound tests instead of a F3. Among the four cleaning solutions examined, the CSM Solution and methanol were the most effective whereas potable water and the Proprietary Solution were the least effective in enhancing PFAS removal and minimizing PFAS rebound from the impacted pipes following the initial rinses. Surprisingly, the Proprietary Solution, which is a commercial product marketed for AFFF cleanout from impacted fire suppression systems, was not significantly more effective than potable water. Aggressive surface agitation via physical scrubbing and ultrasonic cleaning in methanol were demonstrated, in the batch experiments under laboratory settings, to be effective at mitigating the aforementioned PFAS rebound issues. Although these techniques proved effective under laboratory settings, they are not readily implementable in the field. In the flow-through experiments designed to better simulate field conditions employing field-implementable surface agitation techniques, air scouring was ineffective whereas mild heating only provided marginal improvements in enhancing PFAS removal and minimizing PFAS rebound. Therefore, mild heating should be considered during field implementation coupled with aggressive surface agitation techniques including (but not limited to) hot water pressure washing as well as dry ice and sand blasting. Note that several of these techniques might not be applicable to small components of fire suppression systems. Additionally, use of a solid scouring reagent was deemed inappropriate based on our prior correspondence with DoD firetruck operators. Therefore, a prior discussion with

549 and approval from firetruck operators is recommended prior to exploration of these surface

550 agitation techniques in the field.

551   Fluorosurfactants including PFAS are known to self-aggregate into highly

552 thermodynamically stable supramolecular assemblies (e.g., vesicles and lamellar layers)

553 because they contain both highly non-polar fluorinated tails and ionic head groups (Kraft,

554 2001). Specifically, lamellar layers characteristic of PFAS form because fluorosurfactant

555 tails self-aggregate with other non-polar fluorinated tails while the negative charged head

556 groups aggregate around cationic electrolytes in the aqueous solution (Kraft, 2001). The

557 thermodynamic stable nature of these multilayered PFAS assemblies which act a stable

558 crystalline hydrophobic non-aqueous phase is likely attributable to the rebound observed

559 following the initial cleanout of AFFF suppression systems. Indirect, and in select instances,

560 direct observations of these structures were made during SEM and EDX examination of

561 surfaces of impacted pipes. Methanol and the CSM solution were the consistently best

562 performers in solubilizing the fluorosurfactant supramolecular structures and minimizing

563 PFAS rebounds compared to potable water and the Proprietary Solution in this study; this

564 is likely because of the strong PFAS solvency of methanol and the CSM Solution.

565 Diethylene glycol butyl ether (DGBE or butyl carbitol) and propylene glycol are solvents

566 typically found in select AFFF formulations not only because of their strong solvency for

567 PFAS but also their ability to prevent PFAS from forming self-assemblies in AFFF

568 concentrates. Use of chemicals with a strong solvency for PFAS and ability to prevent

569 formation of self-assemblies (Yu et al., 2021) such as diethylene glycol butyl ether (DGBE

570 or butyl carbitol) and propylene glycol (solvents found in select AFFF formulations) may

571 be worth considering in future efforts. Note that management of the PFAS-laden rinsate

572 solutions generated during fire suppression system cleanout represent a secondary source

573 of PFAS contamination that must be properly managed and disposed of; this is an area of

574 active research and should be further explored in future studies.

575 As extensively demonstrated in this study, PFAS rebound following cleanout of AFFF-

576 impacted fire suppression systems is likely inevitable. Without applying aggressive surface

577 agitation techniques that are impractical to implement in the field, substantial PFAS

578 rebound was observed in PFAS-free DI water after the initial triple rinse. It is possible that

579 even more substantial PFAS rebound may occur when these systems are filled with F3s

580 following AFFF cleanout. Due to the difficulty in analyzing for PFAS in F3s, PFAS

581 rebound in F3s was not interrogated as part of this study but must be carefully examined

582 in future studies. Note that a clear understanding of the total PFAS mass present in different

583 components of a fire suppression system or a firefighting equipment is also currently

584 lacking. Therefore, it is recommended that further testing be performed to better understand

585 the nature and extent of PFAS rebound associated with different AFFF-impacted

586 components in a fire suppression system.

587 Collectively, a better understanding of the practical limit to which impacted fire

588 suppression system cleaning can be achieved is needed. However, given the urgent need

589 for F3 transition and replacement, the fire suppression system cleaning/decontamination

590 industry is advancing at a faster pace than the current state of the science and engineering.

591 The lines of evidence employed to validate effective PFAS decontamination by

592 commercial vendors usually only include the concentration of a limited number of target

593 PFAS in solution, as opposed to evaluating all PFAS remaining on impacted surfaces. This

594 approach will not reflect the remaining supramolecular PFAS associated with surfaces and

595   therefore is not a credible line of evidence to demonstrate effective cleaning. The PFAS

596   chosen to be assessed to validate decontamination may also be difficult to justify.

597   Analytical methods such as the EPA Method 1633 only detects a limited number (40) of

598   PFAS target analytes, many of are not the principal fluorosurfactants known to be present

599   in AFFFs (Backe et al., 2013; Place and Field, 2012). Advanced PFAS analytical methods

600   capable of capturing these polyfluoroalkyl fluorosurfactants including the TOP assay and

601   combustion ion chromatography (CIC) provide a more robust alternative to assessing the

602   efficacy of fire suppression system decontamination.

603   Given the extent and magnitude of PFAS rebound following the initial triple rinse

604   observed in this study, improved insights into the dissolution mechanisms and the rate of

605   dissolution of supramolecular formations will likely be key to improving AFFF cleanout

606   processes and decontamination of materials/equipment impacted by PFAS supramolecular

607   formations. While more research is being conducted, practitioners in immediate need of

608   performing AFFF decontamination from fire suppression systems should carefully monitor

609   PFAS rebound immediately following the initial cleanout and thereafter using conventional

610   and advanced PFAS analytical tools. Specifically, short-term (i.e., days) and long-term (i.e.,

611   weeks to months and years) PFAS monitoring should be periodically performed upon

612   completion of AFFF cleanout. With rebound of up to 1.6 g/L of PFAS into F3s following

613   multiple water rinses (Ross, 2019), effective decontamination of fire suppression systems

614   is imperative to i) comply with regulatory thresholds, ii) avoid accidental releases of

615   residual PFAS into the environment, iii) to ensure the safety and firefighting performance

616   of the replacement F3s, and iv) minimize firefighters' exposure to PFAS from handling

617   and training with the next-generation F3.

CRediT Authorship Contribution Statement

Declaration of Competing Interest

Data Availability

Data will be made available upon request.

Acknowledgements

References

641 American Petroleum Institute (API), 2020. Firefighting Foam Transition Guidance.

642 October. https://www.api.org/-/media/files/oil-and-natural-gas/refining/firefighting-

643 foam-transition-guidance-october-2020.pdf

644 Backe, W.J., T.C. Day, and J.A. Field, Zwitterionic, cationic, and anionic fluorinated

645 chemicals in aqueous film forming foam formulations and groundwater from U.S.

646 military bases by nonaqueous large-volume injection HPLC-MS/MS. *Environ Sci*

647 *Technol*, 2013. 47(10): p. 5226-34.

648 Congress, 2020. National Defense Authorization Act for Fiscal Year 2020.

649 https://www.congress.gov/bill/116th-congress/senate-bill/1790

650 Dahlbom, S., Bjarnemark, F., Nguyen, B., Petronis, S. and Mallin, T. 2024. Analysis of

651 per- and polyfluoroalkyl substances (PFAS) extraction from contaminated firefighting

652 materials: Effects of cleaning agent, temperature, and chain-length dependencies.

653 *Emerging Contaminants* 10(3), 100335.

654 Dong D., Kancharla, S., Hooper, J., Tsianou, M., Bedrov, D., Alexandridis, P. 2021.

655 Controlling the Self-Assembly of Perfluorinated Surfactants in Aqueous Environments.

656 *Phys. Chem. Chem. Phys*., 2021,23, 10029-10039.

657 Edwards, D., Appleman, T.D. and Spence, W. 2020 TR-NAVFAC-EXWC-EV-2002:

658 NESDI Project 553 Study of Waste Management and Minimization for AFFF

659 Wastewater.

660 European Union (EU). 2017. COMMISSION REGULATION (EU) 2017/1000 of 13 June

661 2017 amending Annex XVII to Regulation (EC) No 1907/2006 of the European

662 Parliament and of the Council concerning the Registration, Evaluation, Authorisation

663   and Restriction of Chemicals (REACH) as regards perfluorooctanoic acid (PFOA), its

664   salts and PFOA-related substances. Official Journal of the European Union.

665 European Union (EU). 2019. REGULATION (EU) 2019/1021 OF THE EUROPEAN

666   PARLIAMENT AND OF THE COUNCIL. 2019; Available from: https://eur-

667   lex.europa.eu/legal-content/EN/TXT/PDF/?uri=CELEX:32019R1021&from=EN.

668 European Union (EU). 2020. COMMISSION, T.E. COMMISSION DELEGATED

669   REGULATION (EU) 2020/784. 2020; Available from: https://eur-lex.europa.eu/legal-

670   content/EN/TXT/?uri=CELEX:32020R0784.

671 Horst, J., Quinnan, J., McDonough, J., Lang, J., Storch, P., Burdick, J. and Theriault, C.

672   2021. Transitioning Per- and Polyfluoroalkyl Substance Containing Fire Fighting

673   Foams to New Alternatives: Evolving Methods and Best Practices to Protect the

674   Environment. *Groundwater Monitoring & Remediation* 41(2), 19-26.

675 Lang, J.R., McDonough, J., Guillette, T.C., Storch, P., Anderson, J., Liles, D., Prigge, R.,

676   Miles, J.A.L. and Divine, C. 2022. Characterization of per- and polyfluoroalkyl

677   substances on fire suppression system piping and optimization of removal methods.

678   *Chemosphere* 308, 136254.

679 Kostarelos, K., Sharma, P., Christie, E., Wanzek, T., and Field, J. 2020. Viscous

680   Microemulsions of Aqueous Film-Forming Foam (AFFF) and Jet Fuel A Inhibit

681   Infiltration and Subsurface Transport. *Environ. Sci. Technol. Lett*. 2021, 8, 2, 142–147

682 Kraft, M.P. and Riess, J.G. 2009. Chemistry, Physical Chemistry, and Uses of Molecular

683   Fluorocarbon−Hydrocarbon Diblocks, Triblocks, and Related Compounds—Unique

684   "Apolar" Components for Self-Assembled Colloid and Interface Engineering. *Chem.*

685   *Rev*. 2009, 109, 5, 1714–1792.

686   Krafft MP. 2001. Fluorocarbons and fluorinated amphiphiles in drug delivery and
687   biomedical research. *Adv Drug Deliv Rev*. 47(2-3):209-28. doi: 10.1016/s0169-
688   409x(01)00107-7.

689   Marassi, R. and Nobili, F. 2009. Measurement Methods. Structural and Chemical
690   Properties: Scanning Electron Microscopy. Encyclopedia of Electrochemical Power
691   Sources.

692   Miller, C. T., M. M. Poirier-McNeil, and A. S. Mayer (1990), Dissolution of Trapped
693   Nonaqueous Phase Liquids: Mass Transfer Characteristics, *Water Resour. Res*., 26(11),
694   2783–2796, doi:10.1029/WR026i011p02783.

695   Mohona, T.M., Ye, Z., Dai, N., and Nalam, P.C. 2023. Adsorption Behavior of Long-Chain
696   Perfluoroalkyl Substances on Hydrophobic Surface: A Combined Molecular
697   Characterization and Simulation Study. *Water Research*, Volume 239, 120074, ISSN
698   0043-1354, https://doi.org/10.1016/j.watres.2023.120074.

699   Place, B.J. and J.A. Field, Identification of novel fluorochemicals in aqueous film-forming
700   foams used by the US military. *Environ Sci Technol*, 2012. 46(13): p. 7120-7.

701   Powers, S. E., L. M. Abriola, and W. J. Weber Jr. 1994a, An experimental investigation of
702   nonaqueous phase liquid dissolution in saturated subsurface systems: Transient mass
703   transfer rates, *Water Resour. Res*., 30(2), 321–332, doi:10.1029/93WR02923.

704   Powers, S.E., Abriola, L.M., Dunkin, J.S. and Weber, W.J. 1994b. Phenomenological
705   Models for Transient NAPL-Water Mass-Transfer Processes, *Journal of Contaminant*
706   *Hydrology* 16(1); 1-33. https://doi.org/10.1016/0169-7722(94)90070-1.

707   Queensland Department of Environment and Heritage Protection (DOEAHP). 2016.
708   Operational Policy, Environmental Management of Firefighting Foams, in Handout.

709   Queensland Department of Environment and Heritage Protection (DOEAHP). 2017.

710   Environmental Management of Firefighting Foam Policy Explanatory Notes. Available

711   from: https://www.ehp.qld.gov.au/assets/documents/regulation/firefighting-foam-

712   policy-notes.pdf.

713   Riess, J.G.F., F.; Greiner, J.; Krafft, M.P.; Santaella, C.; Vierling, P.; Zarif, L., Membranes,

714   Vesicles, and Other Supramolecular Systems Made from Fluorinated Amphiphiles, in

715   Handbook of Nonmedical Applications of Liposomes From Design to Microreactors,

716   Y.L. Barenholz, D.D., Editor. 1996, CRC Press: Boca Raton.

717   Ross, I. and Storch, P., 2020. Foam Transition: Is it as simple as "foam out/foam in?."

718   *Catalyst*, 1, p.19.

719   Ross, I. 2021. Decontamination of PFAS from fire suppression systems. *Catalysts* Q4, 36-

720   38.

721   Ross, I. 2024. How Clean is Clean? *Catalysts* Q1:56-59.

722   Secretary of Defense for Acquisition and Sustainment 2018   Department of Defense

723   Alternatives to Aqueous Film Forming Foam Report to Congress.

724   Tsianou, M., Bedrov, D., and Alexandridis, P. 2023. Surfactants in the Environment: Self-

725   Assembly of PFAS Pollutants in Solution and at Interfaces. One Hundred Years of

726   Colloid Symposia: Looking Back and Looking Forward. , 443-462. DOI:10.1021/bk-

727   2023-1457.ch016.

728   United States Environmental Protection Agency (EPA). 2024a. Biden-Harris

729   Administration Finalizes Critical Rule to Clean up PFAS Contamination to Protect

730   Public Health. https://www.epa.gov/newsreleases/biden-harris-administration-

731   finalizes-critical-rule-clean-pfas-contamination-protect

732 United States Environmental Protection Agency (EPA). 2024b. Analysis of Per- and

733 Polyfluoroalkyl Substances (PFAS) in Aqueous, Solid, Biosolids, and Tissues Samples

734 by LC-MS/MS. https://www.epa.gov/system/files/documents/2024-01/method-1633-

735 final-for-web-posting.pdf

736 United States Environmental Protection Agency (EPA). 2024c. Final PFAS National

737 Primary Drinking Water Regulation. https://www.epa.gov/sdwa/and-polyfluoroalkyl-

738 substances-pfas

739 United States Department of Defense (DoD). 2023. Performance Specification for Fire

740 Extinguishing Agent, Fluorine-Free Foam (F3) Liquid Concentrate for Land-Based,

741 Fresh Water Applications. https://media.defense.gov/2023/Jan/12/2003144157/-1/-

742 1/1/MILITARY-SPECIFICATION-FOR-FIRE-EXTINGUISHING-AGENT-

743 FLUORINE-FREE-FOAM-F3-LIQUID-CONCENTRATE-FOR-LAND-BASED-

744 FRESH-WATER-APPLICATIONS.PDF

745 Wood, R.J., Sidnell, T., Ross, I., McDonough, J., Lee, J., Bussemaker, M.J. 2020.

746 Ultrasonic Degradation of PFOS Correlated with Sonochemical and Sonoluminescence

747 Characterization. *Ultrasonics Sonochemistry* (68): 105196.

748 Yu, X., Li, F., Fang, H., Miao, X., Wang, J, Zong, R., and Lu, S. 2021. Foaming behavior

749 of fluorocarbon surfactant used in fire-fighting: The importance of viscosity and self-

750 assembly structure. *Journal of Molecular Liquids* (327): 114811.